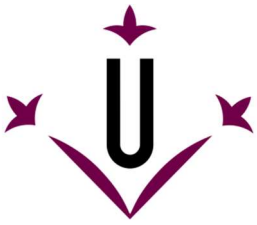

Sprouty1 controls genitourinary development via its N-terminal tyrosine

Marta Vaquero[1], Sara Cuesta[1], Carlos Anerillas[1], Gisela Altés[1], Joan Ribera[1], M. Albert Basson[2], Jonathan D. Licht[3], Joaquim Egea[4], and Mario Encinas[1,*]

Departments of [1]Experimental Medicine and of [4]Basic Medical Sciences, Universitat de Lleida / Institut de Recerca Biomèdica de Lleida, Rovira Roure, 80, Lleida 25198, Spain; [2]Centre for Craniofacial and Regenerative Biology, King's College London, Floor 27, Guy's Hospital, London SE1 9RT, UK; and [3] The University of Florida Health Cancer Center, The University of Florida Cancer/Genetics Research Complex 2033 Mowry Road, Suite 145, Gainesville, FL 32610

[*]To whom correspondence should be addressed:
Mario Encinas, PhD
Department of Experimental Medicine
Universitat de Lleida / Institut de Recerca Biomèdica de Lleida
Edifici Biomedicina I, Lab 2.8
Rovira Roure, 80
Lleida 25198
Spain
Tel/Fax +34-973702951
E-mail: mario.encinas@mex.udl.cat

SIGNIFICANCE STATEMENT

Sprouty1 is a critical regulator of genitourinary development that ensures that only one kidney per side of the embryo is formed. The molecular mechanisms by which Sprouty1 exerts this function are largely unknown. Here we demonstrate that removing a single tyrosine from Sprouty1 in vivo is enough to inactivate its function during genitourinary development. Knockin mice lacking this tyrosine present supernumerary kidneys, megaureter and vesicoureteral reflux, thus phenocopying Sprouty1 knockout mice. These findings shed light on the elusive mechanisms of action of Sprouty proteins, and provide a valuable tool to investigate the developmental origin of human congenital anomalies of kidney and lower urinary tract (CAKUT).

SUMMARY

Background: Congenital anomalies of the kidney and urinary tract (CAKUT) is a group of diseases that include a broad spectrum of developmental defects of the genitourinary system. Mouse models indicate that perturbations of the GDNF-Ret signaling pathway are a major genetic cause of CAKUT. Sprouty1 is an intracellular Ret inhibitor whose mutation results in supernumerary kidneys, megaureters, and hydronephrosis in mice. Both the molecular mechanisms and the structural domains critical for Sprouty function are a matter of controversy, partly because studies pursuing this objective rely on ectopic overexpression in cell lines. A conserved N-terminal tyrosine has been frequently, but not always, identified as critical for their function in vitro.

Methods: We have generated Sprouty1 knockin mice bearing a tyrosine-to-alanine substitution in position 53, corresponding to the conserved N-terminal tyrosine of Sprouty1. We have characterized development of the genitourinary systems of these mice via different methods, including the use of reporter mice expressing EGFP form the Ret locus, and whole mount cytokeratin staining.

Results: Mice lacking this tyrosine grow ectopic ureteric buds that ultimately will form supernumerary kidneys, a phenotype indistinguishable to that of Sprouty1 knockout mice. Sprouty1 knockin mice also present megaureters and vesicoureteral reflux, caused by failure of ureters to separate from Wolffian ducts and migrate to their definitive position.

Conclusions: Tyrosine 53 is absolutely necessary to convey Sprouty1 function during genitourinary development.

Keywords: Sprouty, Ret, Genitourinary Development, Wolffian Duct, Ureteric bud

INTRODUCTION

Congenital anomalies of the kidney and urinary tract (CAKUT) is a group of diseases affecting ~1/500 of human births, and the main cause of pediatric chronic kidney disease. It includes a broad spectrum of developmental defects including renal agenesis, hydronephrosis, vesicoureteral junction obstruction, megaureter, and vesicoureteral reflux[1].

Development of definitive (metanephric) kidneys begins around embryonic day 10.5 (E10.5) with an outgrowth of the Wolffian duct (WD) termed the ureteric bud (UB), that will repeatedly branch to ultimately generate the ureter and the collecting duct system of the kidney. Both the emergence and ulterior branching of the UB are triggered by signals emanating from the receptor tyrosine kinase Ret, which is expressed in the UB epithelium. Ret becomes activated upon binding to its ligand Glial cell line-derived neurotrophic factor (GDNF), secreted by the adjacent metanephric mesenchyme. Knockout mice lacking GDNF, Ret or its co-receptor GFRα1 fail to generate the ureteric bud and consequently die at birth owing to renal agenesis[2]. Later during development, ureters detach from the WD and migrate to their final position at the bladder in a process known as ureter maturation. This remodeling process involves apoptosis of the portion of the WD between the bladder wall and the ureter, known as the common nephric duct (cnd), as well as migration of the distal tip of ureters to their definitive location at the bladder wall [3, 4]. Defective ureter maturation leads to vesicoureteral junction obstruction, hydronephrosis, hydroureter or vesicoureteral reflux. Interestingly, the GDNF-GFRα1-Ret signaling axis is also a major genetic pathway governing ureter maturation [5].

Sprouty family of genes is composed of four members in mammals (Spry1-4), orthologous to a single Drosophila melanogaster gene (dSpry). dSpry gene product is a 63 kDa protein containing a cysteine-rich domain (CRD) in its C-terminus which is conserved across species [6]. Outside the CRD, there is little sequence homology between Sprouty family members, except for a short stretch of aminoacids surrounding a conserved tyrosine (Tyr53 in Spry1), and a serine-rich domain (SRD) present in all four mammalian Sprouty proteins but poorly conserved in dSpry [7].

Genetic experiments in mice clearly establish that Sprouty family members are negative regulators of signaling by Ret during development. Thus, deletion of Spry2 leads to

hyperplasia of the enteric nervous system as a result of excessive Ret signaling [8], whereas Spry1 antagonizes Ret signaling during kidney morphogenesis [9, 10]. Mice deficient in Sprouty1 grow more than one ureteric bud per side of the embryo, thus giving rise to supernumerary kidneys that fuse together into a single anatomic unit. At birth, these animals also present massively dilated ureters (megaureters), multiple cystic cavities inside the kidney parenchyma, and dilation of kidney tubules (hydronephrosis). Epistasis experiments reveal that the underlying cause of such phenotype is excessive activation of the GDNF-GFRα1-Ret signaling axis [9, 11, 12].

Both the molecular mechanisms and the structural domains critical for Sprouty function are far from being understood. The CRD has been shown to be important for homo- and hetero-oligomerization of Spry family members, as well as for translocation to the plasma membrane upon growth factor stimulation. A short stretch of aminoacids within the CRD that bind to Raf-1 have also been shown to be important for Sprouty function. Srpy1 and Spry2 also bind to caveolin-1 through a conserved Arginine located on their carboxy termini [7, 13, 14]. Finally, the role of the conserved tyrosine in the N-terminus of Spry family members (Tyr53 in Spry1) is controversial. Thus, mutation of this tyrosine prevents the ability of Spry proteins to inhibit signaling by receptor tyrosine kinases in some models [15, 16, 17] but fails to do so in others [18]. While these discrepancies may reflect context-specific mechanisms of action of Sprouty proteins, they could also be a consequence of the experimental setting used in these experiments, consisting mainly on ectopic overexpression in cell lines.

To begin to address this question we have generated knockin mice bearing a tyrosine to alanine mutation in residue 53 of Spry1. Analysis of Spry1knockin mice indicate that this tyrosine is absolutely required for Spry1 function during genitourinary (GU) development, as knockin mice faithfully phenocopy CAKUT observed in Spry1 knockout mice. Mice lacking this tyrosine present numerous ectopic UBs along the WD that will ultimately generate supernumerary kidneys. Ureter maturation is also defective in these animals, as ureters fail to detach from the WD and migrate to their final position, leading to vesicoureteral reflux. Finally, a series of internal genitalia malformations likely secondary to ureter maturation defects are also present in Spry1 knockin mice.

METHODS

Mice

All animal use was approved by the Animal Care Committee of the University of Lleida in accordance with the national and regional guidelines. Mice were maintained on a 12h light/dark cycle, and food and water was provided ad libitum. Mice knockout for Spry1 (Spry1$^{tm1.1Jdli}$) were described in [9]. Ret EGFP mice (Ret$^{tm13.1Jmi}$, [19]) were a gift from Dr. Sanjay Jain (Washington University, St Louis, USA). Both knockin and knockout mice used in this paper were on a mixed 50% C57BL/6 x 50% 129Sv genetic background.

Generation of Spry1^{Y53ANeo} knockin mice

The targeting vector consisted of an EcoRI fragment of genomic DNA of approximately 11.5 Kb including the three exons of Spry1, cloned into pBluescript [9]. A change of two nucleotides (TAC to GGC) in the third exon was introduced, converting tyrosine 53 into alanine. A neomycin-resistant cassette flanked by FRT sites was inserted into the BclI site for positive selection. For negative selection, a thymidine kinase (TK) cassette driven by the phosphoglycerate kinase (PGK) promoter was cloned into the SalI site of pBluescript. This vector was linearized with AdhI, and E14 ES cells were electroporated and selected in the presence of 0.250 mg/ml G418 plus 2μM Ganciclovir for 8 days. A total of 508 resistant clones were isolated and grown in 96-well plates. The presence of correctly recombined clones was screened by PCR using primers 396F (5'-GTATAGGAACTTCTGATCATGATGGC-3') and 409R (5'-CACCTAACAAAACCACAAGCTTAAGACC-3'), and a mixture of 30U Taq:1U Pfx (ThermoFisher). Correctly recombined clones yielded a ~4.5 kb band that was resolved in 0.7% agarose gels. Genomic DNA from Spry1 knockout mice was used as a positive control as it was constructed following the same strategy. PCR-positive clones were confirmed by means of Southern Blot. Briefly, genomic DNA was digested overnight with either XbaI (5' arm) or BglII (3' arm). Membranes were hybridized with digoxigenin-labeled probes generated by PCR using the PCR DIG labeling mix (Roche, cat # 1 835 289 910) as per manufacturer's instructions; and primers 390F (5'-ACACAATGGAGGCATTTAAGCAGAA-3') and 391R (5'-ACGGTTATGTGTGGAATTACATGCA-3') for the 5' arm probe and 392F (5'-

CTAACCATTGAGCTACCTCTCCAGCC-3') and 393R (5'-GCTGTGACATAACCCCATGACCAAGG-3') for the 3' arm probe. Blots were developed on X-ray films using CDP* as a substrate (Roche). Two ES clones, 4AD4 and 6DA1, were independently injected to obtain two lines of mice bearing the mutation. The phenotype of these mice was indistinguishable from each other. Most of the results were obtained with the 4AD4 clone. Spry1Y53ANeo mice were genotyped by PCR using primers 429F (5'-TATCAGCCAAGGGTTTCACTACGAG-3'), 430R (5'-TCTAAGAGCACCTCAGAAAGCCAGA-3'), and 431R (5'-CTACCGGTGGATGTGGAATGTGT-3'). After removal of the Neo cassette, Spry1Y53A mice were genotyped using primers 429F and 430R.

Western blot and Immunoprecipitation

Protein extracts from mouse tissues were obtained by mechanical lysis at 4ºC with NP40 buffer (1% Nonidet P-40, 150mM NaCl, 50mM HEPES, 1mM EDTA and 1mM EGTA) supplemented with protease inhibitor cocktail (Roche) and phosphatase inhibitors (1mM NaVO4, 10mM NaF and 50mM β-Glycerophosphate). Western blot was performed as described [20]. For immunoprecipitation, cells were lysed with NP40 buffer supplemented with protease and phosphatase inhibitors as above. Protein was immunoprecipitated overnight at 4ºC with the indicated antibodies plus Protein A/G magnetic beads (Pierce). Antibodies used were as follows: Anti-Spry1 (Cell Signalling, Cat# 13013 for Western blot and Cat# 12993 for immunoprecipitation), Anti β-actin (Santa Cruz, sc-1616), Anti-phosphotyrosine (Millipore, Cat# 05-321), Anti-p53 (Santa Cruz, Cat# sc-126), Anti-$p21^{Cip1}$ (Millipore, Cat# 05-345), Anti-$p19^{Arf}$ (Abcam, Cat# ab80), Anti-Spry2 (Sigma, Cat# S1444).

Subcellular Fractionation and Palmitoylation Assay

Subcellular fractionation was performed using the Subcellular Protein Fractionation Kit for Cultured Cells from Pierce following the manufacturer's instructions. Antibodies used to confirm purity of the fractions included Anti-Caveolin-1 (BD, Cat# 610406), Anti-GAPDH (Abcam, Cat# 8245), Anti-SP-1 (Santa Cruz, Cat# sc-17824) and Anti-Vimentin (BD, Cat# 550513). Palmitoylation assays were performed using the Acyl-RAC pulldown technique

exactly as described [21]. Briefly, after blocking free thiols with methyl methanethiosulfonate (Sigma), lysates are split in half and palmitoyl thioester linkages are cleaved using NH_2OH, or left intact. Newly liberated thiols are captured with thiopropyl Sepharose (Sigma) pulldown, and resolved by SDS-PAGE.

Immunofluorescence and Immunohistochemistry

Frozen sections were blocked with blocking buffer (4% BSA, 1% Triton X-100, 100 mM Glycine in PBS) for 1h at room temperature and incubated with either FITC-DBA (Vector) or Biotin-LTA (Vector) diluted in blocking buffer for an additional hour at RT. Slides containing Biotin-LTA were then incubated with Dylight 594-labeled streptavidin (Jackson Immunoresearch) for 1h at RT. For uroplakin staining, sections were blocked as above and incubated overnight at 4ºC with a rabbit polyclonal antibody (AUM 745) generously provided by Dr. Tung-Tien Sun (New York University). Next day, sections were incubated with Dylight 549-labeled secondary antibodies (Jackson). For WT1 (DAKO) immunohistochemistry, paraffin sections were dewaxed and rehydrated using a xylene/ethanol gradient followed by antigen retrieval (95 °C for 20 min in Tris/EDTA buffer, pH 9) using a PTLink apparatus (DAKO). Staining was performed by an Autostainer device (DAKO). Sections were counterstained with hematoxylin#.

Quantitative RT-PCR

Total RNA was extracted using TRIZOL reagent (ThermoFisher). RNA was reverse transcribed using the High-Capacity cDNA Reverse Transcription Kit (ThermoFisher) as per manufacturer's instructions. Quantitative RT-PCR (qRT-PCR) reactions were performed by means of the SYBR green method, using a 2x Master mix qPCR Low Rox kit (PCR Biosystems). The $2^{-\Delta\Delta Ct}$ method was used, normalizing to actin expression. Reverse transcriptase-minus and blank reactions were included in all experiments. Primers used were as follows: Actin, 616F: 5'-TTCTTTGCAGCTCCTTCGTT-3' and 617R: 5'-ATGGAGGGGAATACAGCCC-3', Spry1, 471F: 5'-CTCTGCGGGCTAAGGAGC-3' and 472R: 5'-ACGCCGGCTGATCTTGC-3'; and Spry2, 620F: 5'-AGAGGATTCAAGGGAGAGGG-3' and 621R: 5'-AGAGGATTCAAGGGAGAGGG-3'.

Whole mount immunofluorescence

For EGFP fluorescence, the GU system of embryos of the indicated ages was dissected and directly photographed under a Nikon SMZ18 fluorescence stereoscope coupled to a Nikon DS-Ri2 camera. For whole mount cytokeratin staining, embryos were fixed overnight at 4ºC in 4% paraformaldehyde. Their GU systems were dissected next day and blocked in blocking buffer (4% BSA, 1% Triton X100,100mM glycine, 0.2% sodium azide in PBS) overnight at 4ºC with gentle agitation. GU systems were then incubated with a 1:100 dilution of anti-cytokeratin antibody (DSHB, TROMA-I) in blocking buffer for 3-5 days at 4ºC. After that, GU systems were washed three times in PBS 1% Triton X100 for 2 hours each at room temperature, and incubated with fluorescently labeled secondary antibodies (Jackson Immunoresearch) in blocking buffer overnight at 4ºC. Tissues were cleared in 1:2 benzyl alcohol:benzyl benzoate (BABB) after being dehydrated through a graded series of methanol. Specimens were placed on coverslips and imaged using a Olympus Fluoview FV1000 confocal laser scanning microscope.

Generation and validation of phospho-Y53 Spry1 specific antibody

The anti-phospho-Y53 Spry1 antibody was produced by Abyntek (Derio, Spain). Rabbits were immunized with the peptide GSNEpYTEGPSVARRPAPRC conjugated to KLH, and antiserum was affinity-purified using the same phosphopeptide. We further purified phospho-antibodies by adsorbing them against the corresponding non-phosphopeptide attached to Aminolink resin (ThermoFisher). 293T cells were transfected with plasmids coding for wild type or Y53A HA-tagged mouse Spry1 by the calcium phosphate method. Before lysis, cells were stimulated or not with 50 ng/ml FGF (Preprotech) for ten minutes. Lysates were subjected to western blot using the pY53 Spry1 purified antibody diluted 1/1000, or antibodies to HA (Sigma, Cat# 00000001186742300), phospho-ERK (Biolegend, Cat# 675502) or Actin (Santa Cruz, Cat# sc-1616).

RESULTS

Generation of Spry1^{Y53ANeo} knockin mice

To explore the role of Spry1 tyrosine 53 in vivo, we generated knockin mice bearing a tyrosine to alanine mutation in this residue. We followed the same strategy used to generate Spry1 knockout mice [9], but the targeting vector lacked loxP sites flanking the Spry1 single coding exon and contained a single nucleotide change generating a Y53A amino acid substitution instead (Figure 1A). ES cells were electroporated with the linearized construct and G418-resistant clones screened for homologous recombination by PCR as described in methods (Figure 1B, top panel). Targeted insertion of both homology arms in PCR-positive clones was confirmed by means of Southern Blot (Figure 1B, middle panel). The presence of the point mutation was confirmed by sequencing. Two independent ES clones, 4AD4 and 6DA1, were used to generate heterozygous knockin mice bearing the Y53A mutation plus the Neo cassette (Spry1$^{Y53ANeo/+}$). We next crossed Spry1$^{Y53ANeo/+}$ animals to obtain knockin mice and examined their offspring. Spry1Y53ANeo/Y53ANeo were born at the expected Mendelian proportions (data not shown). At weaning, knockin mice were slightly smaller than wild type littermates (Figures 1C and 1D), and the number of homozygous mutant females recovered was less than expected, although this trend was not statistically significant (P=0.249 by Chi-Square test) (Figure 1E).

Tyrosine 53 is the major phosphotyrosine of Spry1

Immunoblot analysis revealed that Spry1 was present at slightly increased levels in brains from newborn Spry1$^{Y53ANeo/Y53ANeo}$ when compared to those from wild type littermates (Figure 2A, left panel). Importantly, tissues from knockout mice confirmed the specificity of the Spry1 antibody used. These differences in protein levels were not caused by increased mRNA levels (Figure 2A, right panel). We next analyzed expression of Sprouty1 in E13.5 and newborn kidneys. At both ages, the amount of Sprouty1 was greatly increased in mutant mice (Figures 2B and 2C). Again, mRNA levels were unchanged (Figure 2C, middle panel), indicating that regulation of Sprouty1 levels by tyrosine 53 is post-

transcriptional. Interestingly, levels of Sprouty2 were modestly increased in kidneys from Spry1$^{Y53ANeo/Y53ANeo}$ mice. We next assessed the contribution of Spry1 tyrosine 53 to the global pattern of tyrosine phosphorylation of the protein. Dermal fibroblasts from newborn Spry1$^{Y53ANeo/Y53ANeo}$ mice and wild type littermates were placed in culture and stimulated with sodium pervanadate. After lysis, Spry1 was immunoprecipitated and probed with anti-phosphotyrosine antibodies. Again, skin fibroblasts from Spry1 knockout mice served as negative control. As shown in Figure 3A, pervanadate caused a robust tyrosine phosphorylation of Spry1 that was severely reduced but not completely eliminated upon mutation of tyrosine 53. As expected, no band was found in immunoprecipitates from knockout cells. Thus, tyrosine 53 constitutes a major but not the only phosphorylatable tyrosine of Spry1. To confirm these observations, we generated a phospho-Y53 Spry1 specific antibody. As expected, sodium pervanadate induced a robust phosphorylation of Spry1 immunoprecipitated from fibroblasts from wild type but not Spry1$^{Y53ANeo/Y53ANeo}$ mice (Figure 3B). Specificity of this new anti-phospho-Y53 Spry1 was confirmed using transfected 293T cells (Figure 3C). Finally, we wanted to confirm that mutation of tyrosine 53 does not result in mislocalization of Sprouty1. In agreement with previous studies [22], both wild type and mutant Sprouty1 were localized to the membranous compartments of the cell (Figure 3D), and were palmitoylated (Figure 3E).

Mutation of tyrosine 53 of Spry1 causes genitourinary defects identical to those found in Spry1 knockout mice

Examination of Genitourinary (GU) systems of knockin animals at birth revealed a series of lower urinary tract abnormalities, among which bilateral megaureter was by far the most common. Duplex and blind ureters were also observed, albeit to a much lower incidence. Histologic examination of kidneys revealed that they consisted on two or more supernumerary kidneys fused together, with nephrogenic zones not restricted to the periphery (Figure 4B) that stained positive for the marker Wilms Tumor (WT1) (Figure 5A), large cystic cavities, and hydroureteronephrosis (Figures 4A and 4B). These defects were fully penetrant in homozygous mice, with a small proportion (~10%) of heterozygous mice presenting unilateral megaureter with concomitant kidney defects (Figures 4D and

4E). Moreover, all these abnormalities were indistinguishable from those found in Spry1 knockout mice, indicating that tyrosine 53 is essential for the functions of Spry1 in genitourinary development (Figures 4A and 4B). On the other hand, female Spry1$^{Y53ANeo/Y53ANeo}$ mice presented a series of gross internal genitalia abnormalities at birth including ovaries ectopically placed ventral to the kidneys, with uterine horns attached to ureters and in most cases ending blindly instead of fusing to each other (Figure 4C). Knockin males presented testis set next to kidneys, vasa deferentia were fused to ureters and consequently seminal vesicles were absent (Figure 4C). Again, all these malformations were also found in Spry1 knockout mice [Figure 4A and [9]]. Knockin mice generated from the two independent ES clones presented similar phenotypes. Most of the analyses were performed with the clone 4AD4. Close examination of newborn kidneys from both knockin and knockout mice indicated that the cystic cavities stained positive for the collecting duct marker Dolichos Biflorus Agglutinin (DBA) but not the proximal tubule marker Lotus Tetragonolobus agglutinin (LTA) as previously described [9] (Figure 5B). As expected, hydroureters and swollen renal pelvises stained positive for the urothelium marker uroplakin (Up, Figure 5B).

Aberrant UB development generates supernumerary kidneys in Spry1 knockin mice

It has been previously shown that these urogenital defects are readily rescued by genetically reducing the activation of the GDNF/Ret pathway. Thus, kidney defects found in Spry1 are caused by the emergence of supernumerary, ectopic ureteric buds giving rise to multiplex kidneys owing to hypersensitivity of the WD to GDNF signaling. To further investigate the developmental origin of GU abnormalities of Spry1Y53A knockin mice we crossed Spry1$^{Y53ANeo/+}$ to mice expressing EGFP from the Ret locus[19], thus allowing easy tracking of the WD and the UB (Figure 6A). The UB formed normally in both knockin and knockout mice at E10.5, however several protuberances of the WD cranial to the ureteric bud were observed in mutant but not wild type animals (Figure 6B). At E11.5, a T-shaped ureteric bud had emerged from the WD in wild type mice. At this age the UB of either knockin or knockout mice had also two well-formed branches but the stalk was much shorter than in wild type embryos, and numerous ectopic UBs grew cranially. By E12.5 a

well-developed ureter, completely separated from the WD, and a short common nephric duct (cnd) were present in wild type mice. In contrast, metanephric kidneys from both Spy1$^{Y53ANeo/Y53ANeo}$ and Spry1$^{-/-}$ embryos remained in close proximity to the WD, had many shorter, supernumerary ureteric buds and a much longer cnd (Figure 6B).

Defective ureter maturation causes vesicoureteral reflux, megaureter and internal genitalia defects in Spry1 knockin mice

To image genitourinary development at older embryonic ages we performed whole mount cytokeratin staining as Ret expression gets progressively confined to UB tips and caudal WD, including seminal vesicles, but not ureters ([19] and data not shown). In wild type E12.5 embryos, as observed with EGFP fluorescence, long, completely separated ureters converged with the WD behind a very short cnd. One day later ureters had elongated caudally and cnds were almost eliminated (Figure 7A, left panels). In contrast, at E12.5 knockin mice presented an flat, triangle-shaped structure [Figure 7A, top right panel (arrow)], that was continuous with in a very long cnd on its caudal side. At E13.5 kidneys from knockin mice were caudally misplaced, in close proximity to this enlarged planar structure (Figure 7A, bottom right panel), to where both multiple UBs and the WD were connected (Figure 7B). At E15.5, numerous ectopic kidneys arising at different points of the Wolffian duct and that attached together to form a single anatomic unit were present in knockin mice (Figure 7D). Each of these supernumerary kidneys had an ureter that, together with the WD, fused to the flat triangle-shaped structure, which was continuous with a greatly enlarged cnd, acquiring the shape of a megaureter (Figure 7C, arrows). At this age, ureter maturation had proceeded completely in wild type animals, with ureters completely segregated from the WD. Ureters connected to the bladder at their definitive location (Figure 7E, arrowheads), whereas WDs remained attached to the pelvic urethra (Figure 7E, asterisks). Ureter maturation never happened in mutant mice, thus leaving WD and ureters fused together and connecting to the pelvic urethra (Figure 7E). Such broad, ectopic insertion precluded correct formation of the vesicoureteral junction, giving rise to vesicoureteral reflux as demonstrated by trypan blue injection into the bladder (Figure 7D, bottom panel). This observation explains both the presence of urine-filled megaureters and

hydroureteronephrosis found in newborn mutant mice. On the other hand, Müllerian ducts failed to fuse to each other at the midline but instead coiled around giving rise to blind uterine horns found in newborn mice (Figure 7D, top panel). Finally, failure or ureters to segregate from WD cause fusion of vasa deferentia to ureters in newborn mutant males.

In conclusion, we have demonstrated that mutation of the N-terminal tyrosine of Sprouty1 leads to formation of ectopic ureteric buds that ultimately will form supernumerary kidneys, thus phenocopying Spry1 knockout mice. A more detailed analysis of ureter maturation reveals a series of defects that eventually lead to formation of megaureters and vesicoureteral reflux.

DISCUSSION

Phosphorylation of the conserved N-terminal tyrosine is the most abundant post-translational modification (PTM) detected in Sprouty family members, representing 63-77% of total PMTs found in high-throughput proteomic experiments [PhosphositePlus [23]]. Accordingly, we have found that tyrosine 53 is the major (but not the only) phosphotyrosine in mouse Sprouty1. Besides tyrosine 53, the same high-throughput experiments have identified two extra phosphotyrosines in Sprouty1, namely tyrosine 89 (identified 50 times vs. 247 times for tyrosine 53) and tyrosine 304 (7 times). The function of these tyrosines is essentially unexplored and deserves future investigation. Other C-terminal tyrosines found in Sprouty2 such as tyrosines 227, 269 and 283 [24] have not being identified on its phosphorylated form in Sprouty1.

We have found that knockin mice lacking tyrosine 53 phenocopy the renal malformations found in Spry1$^{-/-}$ mice, namely emergence of ectopic UBs leading to supernumerary kidneys. The role of the conserved N-terminal tyrosine of Sprouty proteins has been previously tested by several independent laboratories, essentially in the context of Extracellular-signal regulated kinase (ERK) pathway inhibition —regarded as the primary target of Sprouty proteins. While some studies showed that mutation of that tyrosine renders Sprouty proteins unable to block the ERK pathway [17], [16], [15], others have found that its phosphorylation is dispensable for inhibition of the pathway [18]. These discrepancies might be related to differences in the context in which these experiments were conducted, including the cell type, the growth factors used, or the family member(s) analyzed, but also can reflect two distinct modes of action of these proteins. Thus, in experimental paradigms where Sprouty proteins act at the level of Raf-1 [25], [18], phosphorylation of this tyrosine would be dispensable for their function, whereas in models where Sprouty proteins act upstream of Ras [16], [15], this tyrosine would be absolutely necessary for their activity. Our data clearly show that tyrosine 53 of Spry1 is essential for its function at least in the context of genitourinary development, favoring the second model. However, we cannot rule out the possibility that in other cellular systems mutation of tyrosine 53 would have no effect on the activity of Spry1.

We also describe ureter maturation defects in our mutant mice, essentially consisting on failure of the ureters to elongate, to properly separate from the WD and therefore to migrate to their definitive insertion at the bladder. It has been previously described that excessive activation of the ERK pathway in the developing lung leads to aberrant mitotic spindle orientation and abnormal airway shape [26]. We hypothesize that the same mechanism would explain the some of the above defects. Thus, in mutant mice epithelial cells from the UBs would not undergo mitotic divisions oriented parallel to the longitudinal axis of the ureter, but rather place their mitotic spindles in a disorganized fashion, leading to the appearance of the flat, triangle-shaped structure connecting UBs and WD. In parallel, the cnd fails to degenerate and ends up forming the caudal part of the ectopically inserted megaureters found in Spry1 mutant mice. It has been previously shown that degeneration of the cnd by apoptosis is crucial for proper ureter detachment from the WD during ureter maturation [3, 4]. On the other hand, increased ERK activity in Ret Y1015F mutants leads to decreased apoptosis of the cnd [19]. Finally, these ureter maturation defects are rescued by genetically reducing the activation of the GDNF-Ret signaling pathway [9], [11], [12]. Altogether, these observations strongly suggest that mutation of Sprouty1 leads to an increase of Ret-derived ERK phosphorylation, that in turns inhibits apoptosis of the cnd.

Mechanistically, how deletion of the N-terminal tyrosine blocks Sprouty function is still a matter of debate. It was initially described that this phosphotyrosine provides a binding site for the SH2 domain of Grb2, and therefore sequestering of this adaptor by Sprouty proteins upon growth factor stimulation would uncouple RTK phosphorylation from ERK pathway activation [16]. However, later on it was shown that association of Grb2 to Sprouty was independent of tyrosine phosphorylation [15]. Perhaps the most widely accepted protein binding this phosphotyrosine is the ubiquitin ligase c-Cbl. According to one model Spry2 sequesters c-Cbl away from the EGFR, thus blocking its proteasomal degradation and potentiating signaling by EGF [27], [28], [29], [30]. However, such mechanism obviously only operates in systems where Spry2 activates instead of inhibits EGFR signaling, but won't explain how this tyrosine inhibits signaling by FGFR or Ret. In a more general scenario, the functional consequence of binding of c-Cbl to Spry2 is proteasomal degradation of the latter [31], [27], [15]. Our data are in agreement with these observations, as steady-state levels of Spry1 are increased in brain lysates from Spry1$^{Y53A/Y53A}$ mice when compared to their wild

type littermates. However, attenuation of FGF-mediated ERK phosphorylation by Spry2 is not dependent on c-Cbl, as Spry2 efficiently inhibits ERK phosphorylation in MEFs from c-Cbl$^{-/-}$ mice [15]. In conclusion, the mechanisms by which the N-terminal tyrosine of Sprouty proteins mediate their function require further investigation. We believe that our Spry1Y53A knockin mouse represents an excellent model system to pursue this objective.

AUTHOR CONTRIBUTIONS

Conceptualization, ME; Methodology, JE, ME; Investigation, MV, CA, SC, JE, JR, GA, ME; Resources, MAB, JDL; Writing–original draft, ME; Writing–Review & Editing, MV, CA, MAB, JDL, JE; Visualization, MV, CA, ME; Supervision, ME; Funding Acquisition, ME.

ACKNOWLEDGEMENTS

The authors declare no competing interests. This work was supported by grants BFU2010-47175-P and BFU2017-83646-P (AEI/FEDER, UE) from MINECO to ME. MV was supported by a predoctoral fellowship from AGAUR. CA was supported by a predoctoral fellowship from Universitat de Lleida. SC was supported by a Cofund action from the Marie Curie program of the EU. We are grateful to Dr. Sanjay Jain (Washington University, St Louis) for sharing Ret^{EGFP} mice, and to Dr. Tung-Tien Sun (New York University) for Uroplakin antibody. We thank Anna Macià (IRB Lleida) for her contribution to the initial development of this manuscript, as well as Marta Hereu, Maria Santacana, Mónica Domingo and Maria Carrele for their excellent technical assistance.

REFERENCES

1. Schedl A: Renal abnormalities and their developmental origin. *Nat. Rev. Genet.* 8: 791–802, 2007

2. Davis TK, Hoshi M, Jain S: To bud or not to bud: the RET perspective in CAKUT. *Pediatr. Nephrol.* 29: 597–608, 2014

3. Batourina E, Tsai S, Lambert S, Sprenkle P, Viana R, Dutta S, Hensle T, Wang F, Niederreither K, McMahon AP, Carroll TJ, Mendelsohn CL: Apoptosis induced by vitamin A signaling is crucial for connecting the ureters to the bladder. *Nat. Genet.* 37: 1082–9, 2005

4. Uetani N, Bertozzi K, Chagnon MJ, Hendriks W, Tremblay ML, Bouchard M: Maturation of ureter-bladder connection in mice is controlled by LAR family receptor protein tyrosine phosphatases. *J. Clin. Invest.* 119: 924–35, 2009

5. Uetani N, Bouchard M: Plumbing in the embryo: developmental defects of the urinary tracts. *Clin. Genet.* 75: 307–317, 2009

6. Hacohen N, Kramer S, Sutherland D, Hiromi Y, Krasnow MA: sprouty encodes a novel antagonist of FGF signaling that patterns apical branching of the Drosophila airways. *Cell* 92: 253–263, 1998

7. Guy GR, Jackson RA, Yusoff P, Chow SY: Sprouty proteins: modified modulators, matchmakers or missing links? *J Endocrinol* 203: 191–202, 2009

8. Taketomi T, Yoshiga D, Taniguchi K, Kobayashi T, Nonami A, Kato R, Sasaki M, Sasaki A, Ishibashi H, Moriyama M, Nakamura K, Nishimura J, Yoshimura A: Loss of mammalian Sprouty2 leads to enteric neuronal hyperplasia and esophageal achalasia. *Nat Neurosci* 8: 855–857, 2005

9. Basson MA, Akbulut S, Watson-Johnson J, Simon R, Carroll TJ, Shakya R, Gross I, Martin GR, Lufkin T, McMahon AP, Wilson PD, Costantini FD, Mason IJ, Licht JD: Sprouty1 is a critical regulator of GDNF/RET-mediated kidney induction. *Dev Cell* 8: 229–239, 2005

10. Basson MA, Watson-Johnson J, Shakya R, Akbulut S, Hyink D, Costantini FD, Wilson PD, Mason IJ, Licht JD: Branching morphogenesis of the ureteric epithelium during kidney development is coordinated by the opposing functions of GDNF and Sprouty1. *Dev Biol* 299: 466–477, 2006

11. Rozen EJ, Schmidt H, Dolcet X, Basson MA, Jain S, Encinas M: Loss of Sprouty1 rescues renal agenesis caused by ret mutation. *J. Am. Soc. Nephrol.* 20: 2009

12. Michos O, Cebrian C, Hyink D, Grieshammer U, Williams L, D'Agati V, Licht JD, Martin GR, Costantini F: Kidney development in the absence of Gdnf and Spry1 requires Fgf10. *PLoS Genet* 6: e1000809, 2010

13. Cabrita MA, Christofori G: Sprouty proteins, masterminds of receptor tyrosine kinase signaling. *Angiogenesis* 11: 53–62, 2008

14. Edwin F, Anderson K, Ying C, Patel TB: Intermolecular interactions of Sprouty proteins and their implications in development and disease. *Mol Pharmacol* 76: 679–691, 2009

15. Mason JM, Morrison DJ, Bassit B, Dimri M, Band H, Licht JD, Gross I: Tyrosine Phosphorylation of Sprouty Proteins Regulates Their Ability to Inhibit Growth Factor Signaling: A Dual Feedback Loop. *Mol. Biol. Cell* 15: 2176–2188, 2004

16. Hanafusa H, Torii S, Yasunaga T, Nishida E: Sprouty1 and Sprouty2 provide a control mechanism for the Ras/MAPK signalling pathway. *Nat Cell Biol* 4: 850–858, 2002

17. Sasaki A, Taketomi T, Wakioka T, Kato R, Yoshimura A: Identification of a dominant negative mutant of Sprouty that potentiates fibroblast growth factor- but not epidermal growth factor-induced ERK activation. *J Biol Chem* 276: 36804–36808, 2001

18. Sasaki A, Taketomi T, Kato R, Saeki K, Nonami A, Sasaki M, Kuriyama M, Saito N, Shibuya M, Yoshimura A: Mammalian Sprouty4 suppresses Ras-independent ERK activation by binding to Raf1. *Nat Cell Biol* 5: 427–432, 2003

19. Hoshi M, Batourina E, Mendelsohn C, Jain S: Novel mechanisms of early upper and lower urinary tract patterning regulated by RetY1015 docking tyrosine in mice. *Development* 139: 2405–2415, 2012

20. MacIà A, Vaquero M, Gou-Fàbregas M, Castelblanco E, Valdivielso JM, Anerillas C, Mauricio D, Matias-Guiu X, Ribera J, Encinas M: Sprouty1 induces a senescence-associated secretory phenotype by regulating NFκB activity: Implications for tumorigenesis. *Cell Death Differ.* 21: 2014

21. Forrester MT, Hess DT, Thompson JW, Hultman R, Moseley MA, Stamler JS, Casey PJ: Site-specific analysis of protein S-acylation by resin-assisted capture. *J. Lipid Res.* 52: 393–8, 2011

22. Impagnatiello MA, Weitzer S, Gannon G, Compagni A, Cotten M, Christofori G: Mammalian sprouty-1 and -2 are membrane-anchored phosphoprotein inhibitors of growth factor signaling in endothelial cells. *J. Cell Biol.* 152: 1087–98, 2001

23. Hornbeck P V, Zhang B, Murray B, Kornhauser JM, Latham V, Skrzypek E: PhosphoSitePlus, 2014: mutations, PTMs and recalibrations. *Nucleic Acids Res.* 43: D512-20, 2015

24. Rubin C, Zwang Y, Vaisman N, Ron D, Yarden Y: Phosphorylation of Carboxyl-terminal Tyrosines Modulates the Specificity of Sprouty-2 Inhibition of Different Signaling Pathways. *J. Biol. Chem.* 280: 9735–9744, 2005

25. Yusoff P, Lao DH, Ong SH, Wong ES, Lim J, Lo TL, Leong HF, Fong CW, Guy GR: Sprouty2 inhibits the Ras/MAP kinase pathway by inhibiting the activation of Raf. *J Biol Chem* 277: 3195–3201, 2002

26. Tang N, Marshall WF, McMahon M, Metzger RJ, Martin GR: Control of Mitotic Spindle Angle by the RAS-Regulated ERK1/2 Pathway Determines Lung Tube

Shape. *Science (80-.).* 333: 342–345, 2011

27. Rubin C, Litvak V, Medvedovsky H, Zwang Y, Lev S, Yarden Y: Sprouty Fine-Tunes EGF Signaling through Interlinked Positive and Negative Feedback Loops. *Curr. Biol.* 13: 297–307, 2003

28. Fong CW, Leong HF, Wong ESM, Lim J, Yusoff P, Guy GR: Tyrosine phosphorylation of Sprouty2 enhances its interaction with c-Cbl and is crucial for its function. *J. Biol. Chem.* 278: 33456–64, 2003

29. Wong ESM, Fong CW, Lim J, Yusoff P, Low BC, Langdon WY, Guy GR: Sprouty2 attenuates epidermal growth factor receptor ubiquitylation and endocytosis, and consequently enhances Ras/ERK signalling. *EMBO J.* 21: 4796–808, 2002

30. Egan JE, Hall AB, Yatsula BA, Bar-Sagi D: The bimodal regulation of epidermal growth factor signaling by human Sprouty proteins. *Proc. Natl. Acad. Sci. U. S. A.* 99: 6041–6, 2002

31. Hall AB, Jura N, DaSilva J, Jang YJ, Gong D, Bar-Sagi D: hSpry2 is targeted to the ubiquitin-dependent proteasome pathway by c-Cbl. *Curr. Biol.* 13: 308–14, 2003

FIGURE LEGENDS

Figure 1. Generation of Spry1 Y53A knockin mice. (A) Targeting strategy used, including primers used for PCR screening and genotyping, and southern blot probes (black horizontal bars). (B) A first screening was performed using by PCR using primers 396F and 409R (top panel). Tail DNA from $Spry1^{-/-}$ mice served as positive control. PCR-positive clones (asterisk) were confirmed by southern blot (middle panel), and $Spry^{Y53ANeo/+}$ mice were genotyped using primers 429F, 430R and 431R (lower panel). (C, D) Reduced weight of male and female knockin mice at weaning. P-values were calculated by the Mann-Whitney test. (E) Allelic frequencies at weaning (3-4 weeks).

Figure 2. Expression of wild type and mutant Sprouty1. (A) Levels of Spry1 from newborn brains of the indicated genotypes were measured by western blot (left panel). Right panel, quantification of protein and mRNA levels from newborn brains of the indicated genotypes. Equal mRNA levels indicate that regulation of protein levels by tyrosine 53 is post-transcriptional. Asterisk denotes P=0.11 by Mann-Whitney test. (B) Protein levels of E13.5 kidneys from the indicated genotypes. Note much higher levels in knockin metanephroi. (C) Sprouty1 protein and mRNA levels of newborn kidneys from the indicated genotypes. Short and long exposures of Sprouty1 immunoblots are shown to illustrate the difference between genotypes. Levels of Sprouty2 are included for comparison. The number in parentheses indicate sample number in all graphs.

Figure 3. Characterization of Spry1 Y53A protein. (A, B) Spry1 was immunoprecipitated from pervanadate-stimulated skin fibroblasts of the depicted genotypes, and membranes probed with the indicated antibodies. NS, non-specific band. IgG-L and IgG-H, low molecular and high molecular weight immunoglobulin chains. (C) Validation of phospho-Y53 Spry1 antibody. 293T cells were transfected with empty vector or plasmids coding for HA-tagged wild type or Y53A mouse Spry1. Cells were stimulated or not with FGF for 10 min, lysed and resolved by SDS-PAGE. Membranes were incubated with the indicated antibodies. Note that overexpression of Sprouty1 in 293T cells leads to

constitutive phosphorylation of tyrosine 53. (D) Subcellular fractionation of skin fibroblast extracts indicates that both wild type and Y53A Sprouty1 proteins localize to the membranous fraction of the cell. GAPDH, Caveolin-1, SP-1 and vimentin are markers of Cytosolic (Cyto), Membranous (Memb), Nuclear (Nuc) and Cytoskeletal (Cskel) fractions, respectively. (E) Both wild type and Y53A Sprouty1 are palmitoylated. The presence of a band in the NH_2OH-treated lysates from skin fibroblasts indicates palmitoylation of the protein (see methods for details).

Figure 4 . Spry1$^{Y53ANeo/Y53ANeo}$ phenocopy Spry1$^{-/-}$ mice in terms of genitourinary development. (A) Gross anatomy of newborn GU from the indicated genotypes (top panel). Hematoxylin-eosin stained sections of newborn kidneys of the indicated genotypes (middle panel). (B) Higher magnification of sections from the indicated genotypes showing ectopic nephrogenic zones and cystic cavities. Scale bar, 100 μm. (C) Detail of some GU abnormalities found in Spry1$^{Y53ANeo/Y53ANeo}$ mice including duplex ureters (left), blind uterine horns (middle) and vasa deferentia fused to ureters (right). (D) Unilateral CAKUT present in ~10% of Spry1$^{Y53ANeo/+}$ mice. (E) Quantification of GU defects found in newborn mice of the indicated genotypes. Ad, adrenal gland; K, kidney; Ov, ovary; T, testis; Ur, ureter; Ut, uterus; Vd, vas deferens.

Figure 5. Characterization of kidneys from newborn Spry1 knockin and knockout mice. (A) Wilms Tumor (WT1) staining of the ectopic nephrogenic zones. Note WT1-positive developing and mature nephrons, but not cystic cavities (B) Dolichos Biflorus Agglutinin (DBA) and Lotus Tetragonolobus agglutinin (LTA) and uroplakin (Up) staining of newborn kidneys from the indicated genotypes. Cysts are DBA-positive, revealing their collecting duct origin. Scale bars: 200 μm for 4x and 20 μm for 40x pictures.

Figure 6. Aberrant ureteric bud development in Spry1 Y53A mice is indistinguishable to that of and Spry1 knockout mice. (A) Diagram showing Ret and Spry1 loci and mouse crosses to generate genotypes of interest. (B) EGFP fluorescence of UB and WD

development from embryos of the indicated ages and genotypes (all of them bearing one Ret^{EGFP} allele to allow visualization of these structures). Note ectopic UBs (arrowheads) and long common nephric ducts (cnd, brackets) in both Spry1 knockin and knockout mutant mice. WD, Wolffian duct.

Figure 7. Ureter maturation defects leading to vesicoureteral reflux in Spry1 knockin mice. (A) Whole mount cytokeratin staining of embryonic GU system of the indicated ages and genotypes. Note long cnd and the presence of a flat, triangle-shaped structure connecting WD, UBs and cnd in mutant mice (arrow). Also note failure of kidneys to migrate away from the point at which WD and UBs converge. G, gut. (B) Detail of E13.5 mutant GU stained with cytokeratin. Confocal stacks were divided in ventral (Z1) and dorsal (Z2) sections and pseudocolored in green and red for clarity. Note how the WD (arrowheads) is continuous with the triangle-shaped structure (arrow) and the ureter (asterisk). Note also how ectopic UBs integrate into one kidney. (C) Cytokeratin staining of GU systems from E15.5 embryos. The triangle-shaped structure (arrow) is continuous with an enlarged cnd, and together from a megaureter. MD, Müllerian duct. (D) Stereoscope image of knockin female GU shown in C allows clear visualization of supernumerary kidneys (K1 to K5) and ureters (Ur1 to Ur5) (E) Top panel: Detail of C showing complete separation between ureters (Ur), which insert into the bladder (Bl, arrowheads) and WDs, which join the pelvic urethra (PUr) at the points marked with asterisks, in wild type embryos. In knockin embryos, the cnd insert directly into the PUr. Note the Müllerian ducts (MD, arrows) coiling around instead of fusing to each other at the midline. Bottom panel, injection of trypan blue into the bladder of wild type and mutant dissected GU from newborn mice show vesicoureteral reflux in the latter.

Figure 1. Vaquero et al.

A

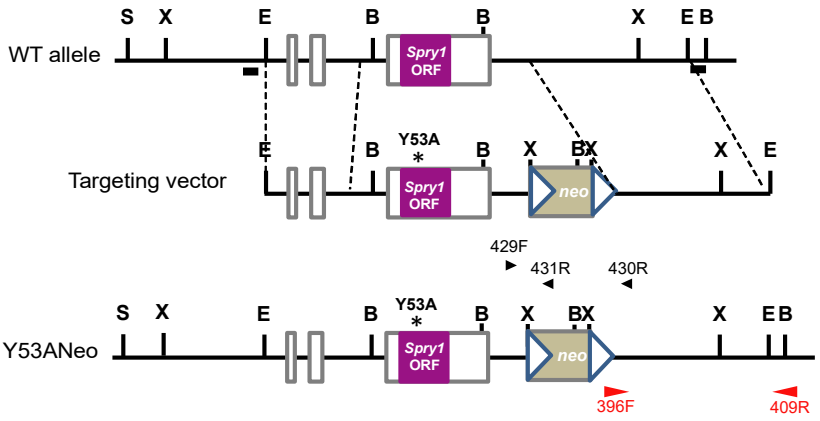

B

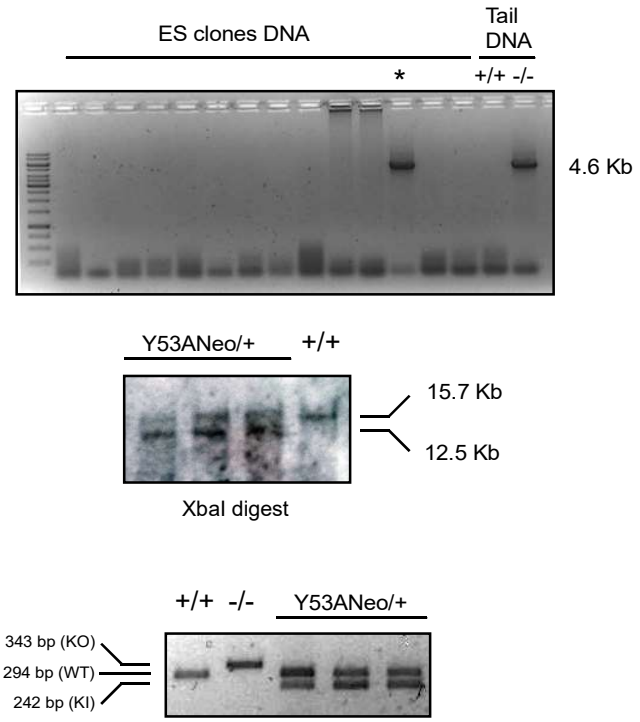

C

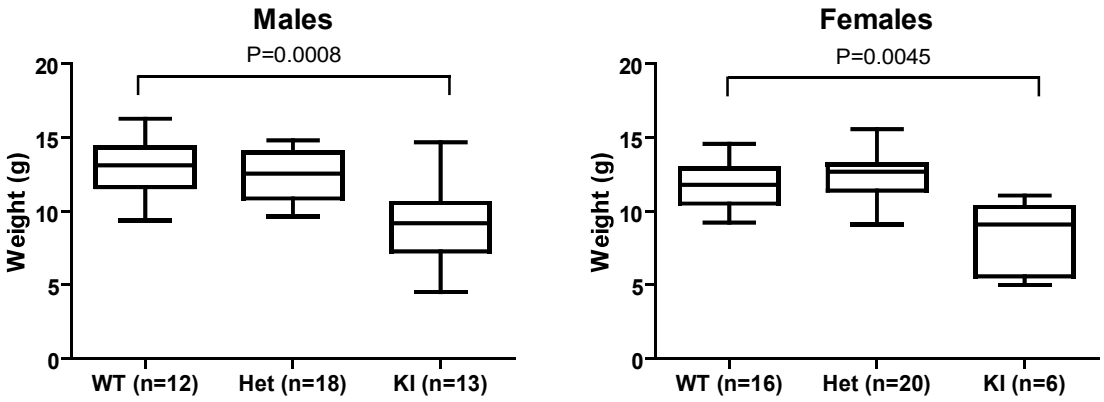

D

E

Females	Expected	Observed
Spry1 $^{+/+}$	11	17
Spry1 $^{Y53A/+}$	21	20
Spry1 $^{Y53A/Y53A}$	11	6
Total	43	43

Males	Expected	Observed
Spry1 $^{+/+}$	12.5	13
Spry1 $^{Y53A/+}$	25	23
Spry1 $^{Y53A/Y53A}$	12.5	14
Total	50	50

A

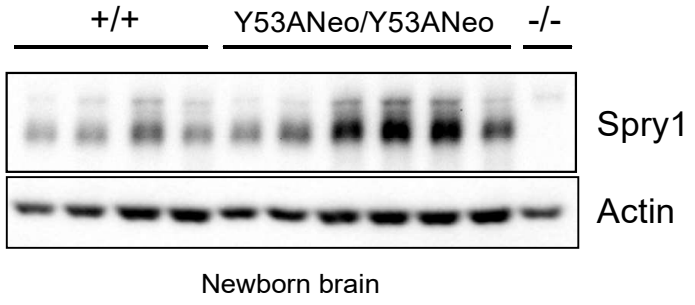
+/+
Y53ANeo/Y53ANeo
-/-
Spry1
Actin
Newborn brain

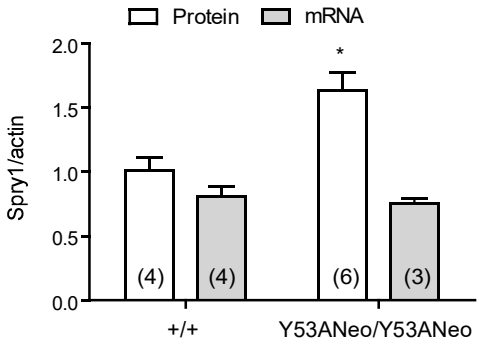
Protein
mRNA
Spry1/actin
2.0
1.5
1.0
0.5
0.0
*
(4)
(4)
(6)
(3)
+/+
Y53ANeo/Y53ANeo

B

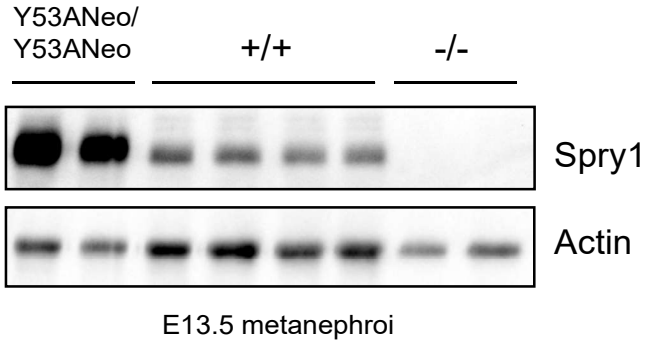
Y53ANeo/
Y53ANeo
+/+
-/-
Spry1
Actin
E13.5 metanephroi

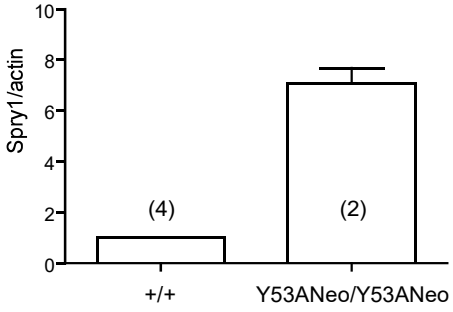
Spry1/actin
10
8
6
4
2
0
(4)
(2)
+/+
Y53ANeo/Y53ANeo

C

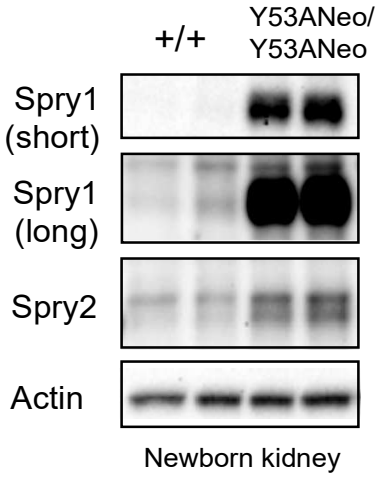
+/+
Y53ANeo/
Y53ANeo
Spry1
(short)
Spry1
(long)
Spry2
Actin
Newborn kidney

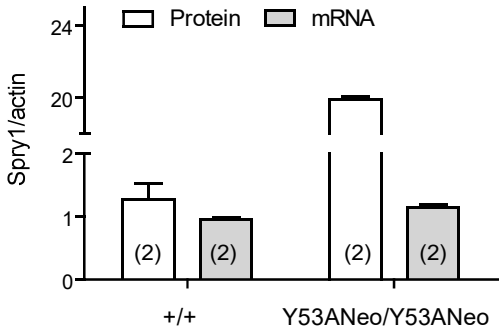
Protein
mRNA
Spry1/actin
24
20
2
1
0
(2)
(2)
(2)
(2)
+/+
Y53ANeo/Y53ANeo

Figure 3. Vaquero et al.

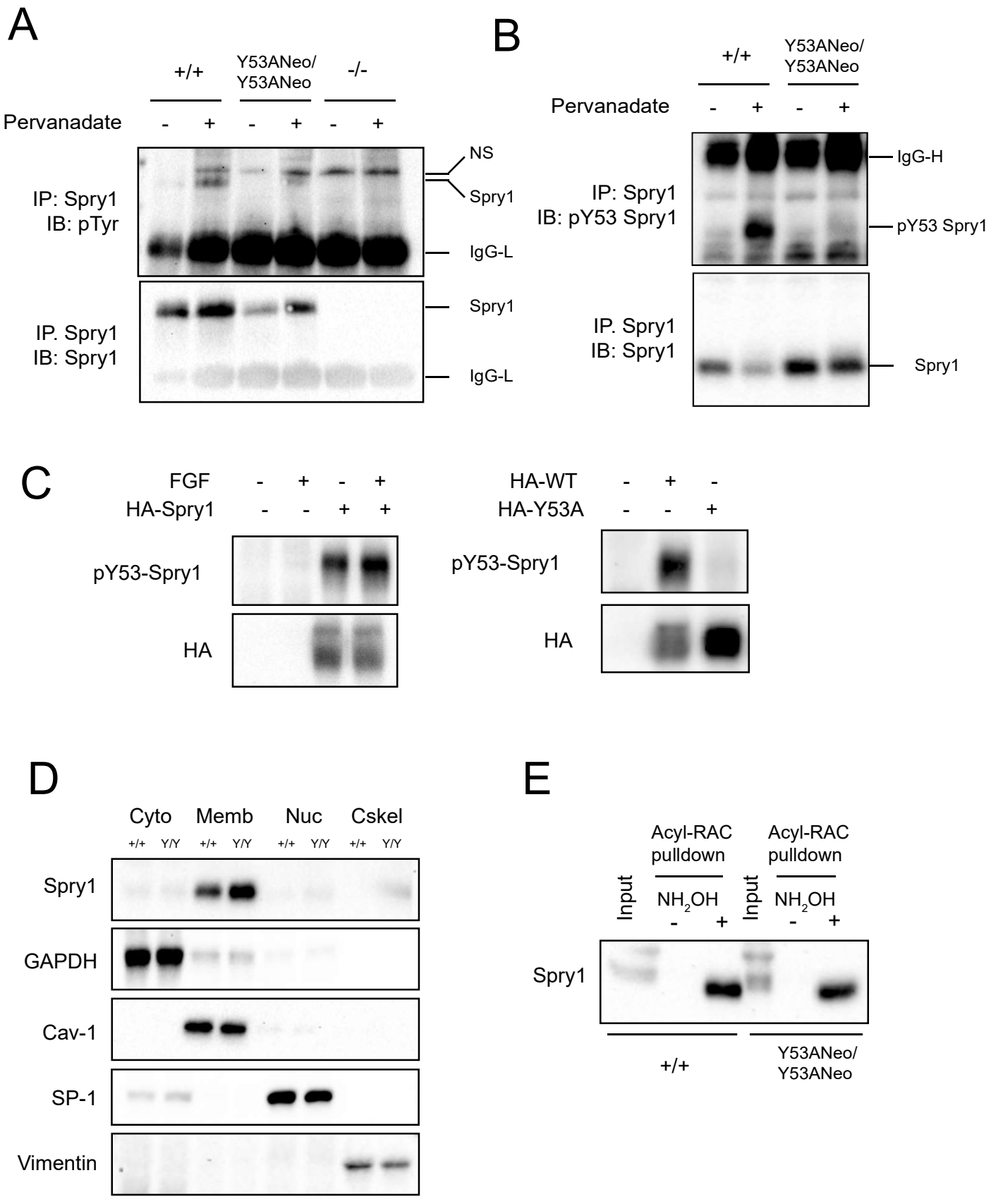

Figure 4. Vaquero et al.

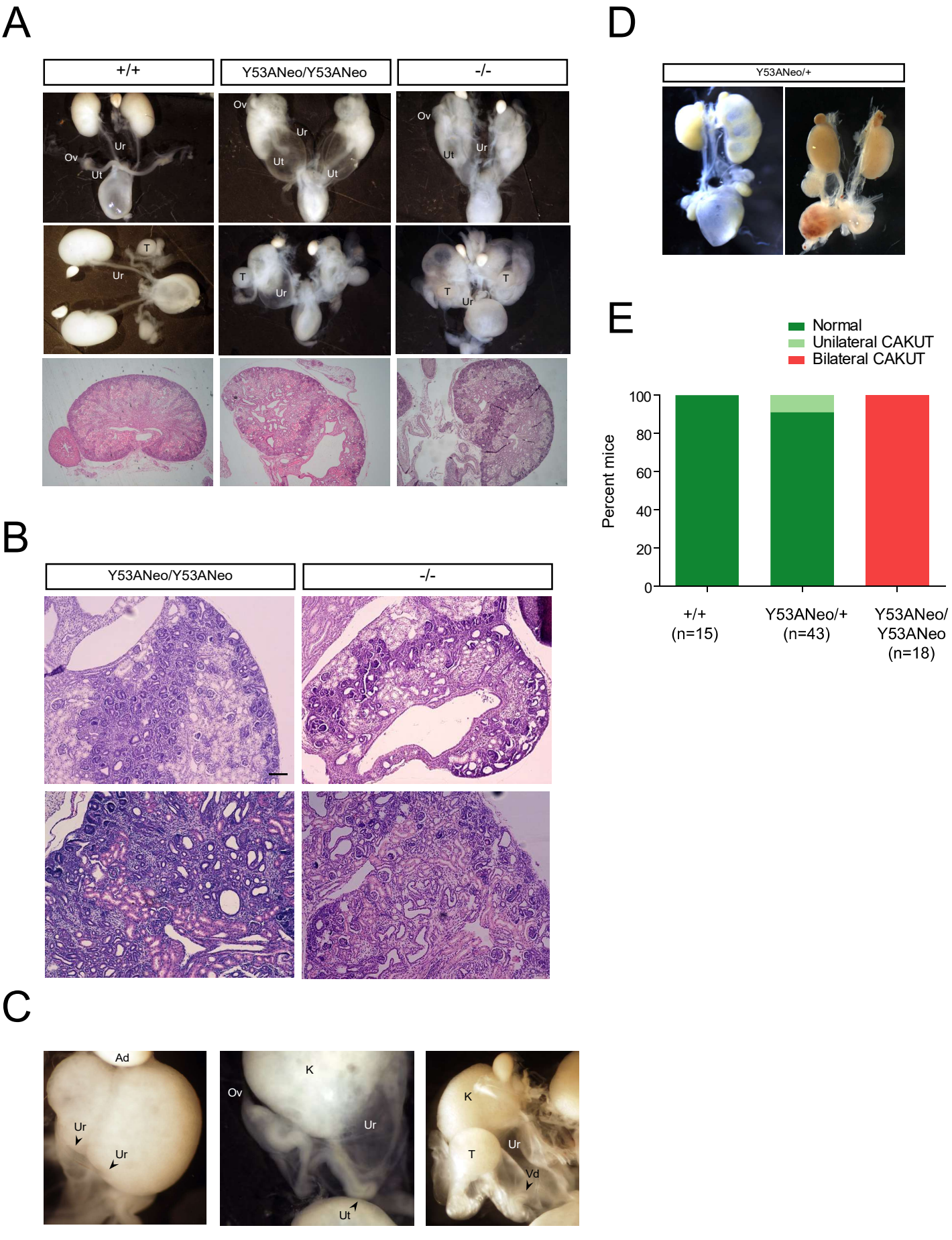

Figure 5. Vaquero et al.

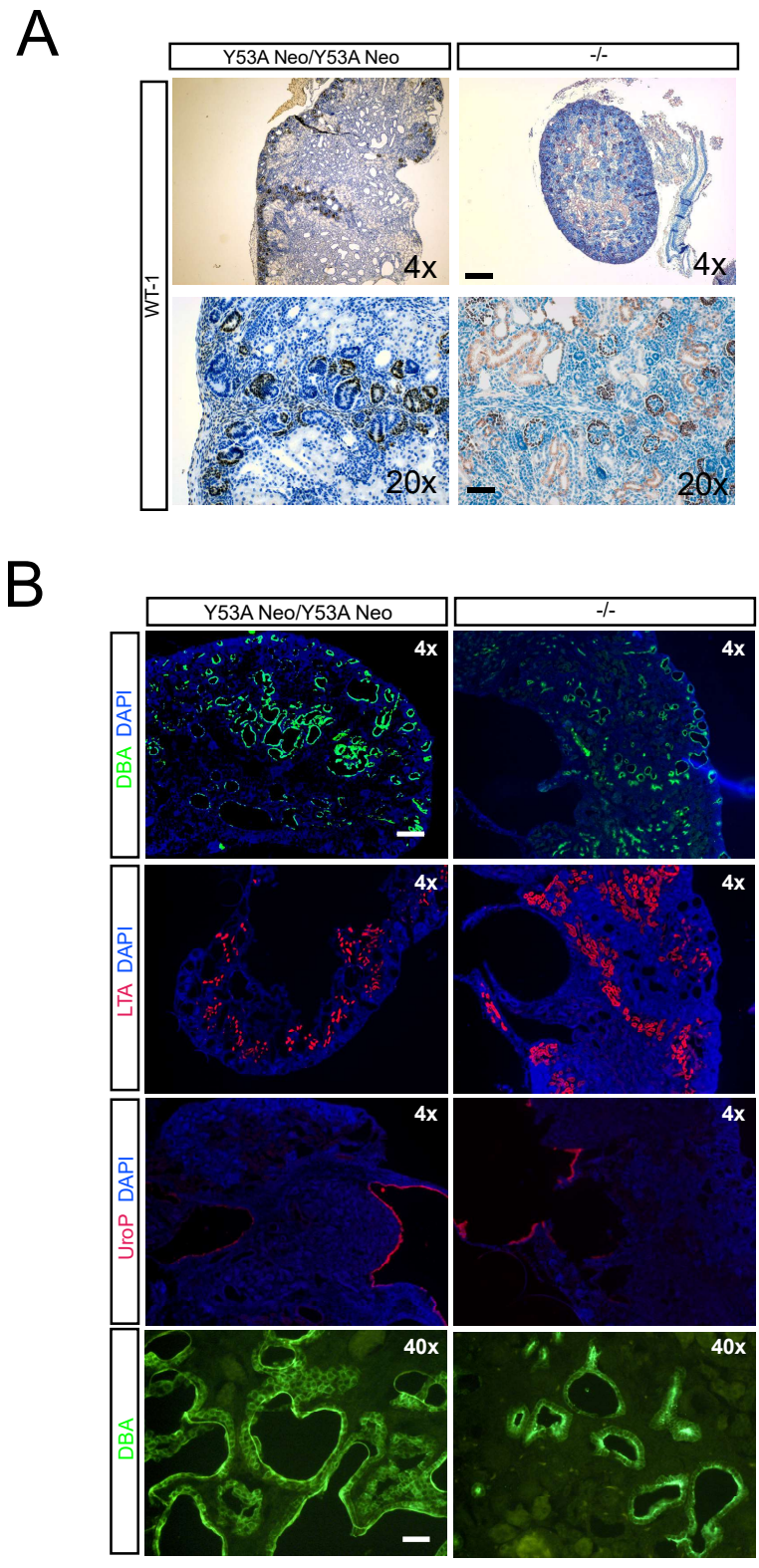

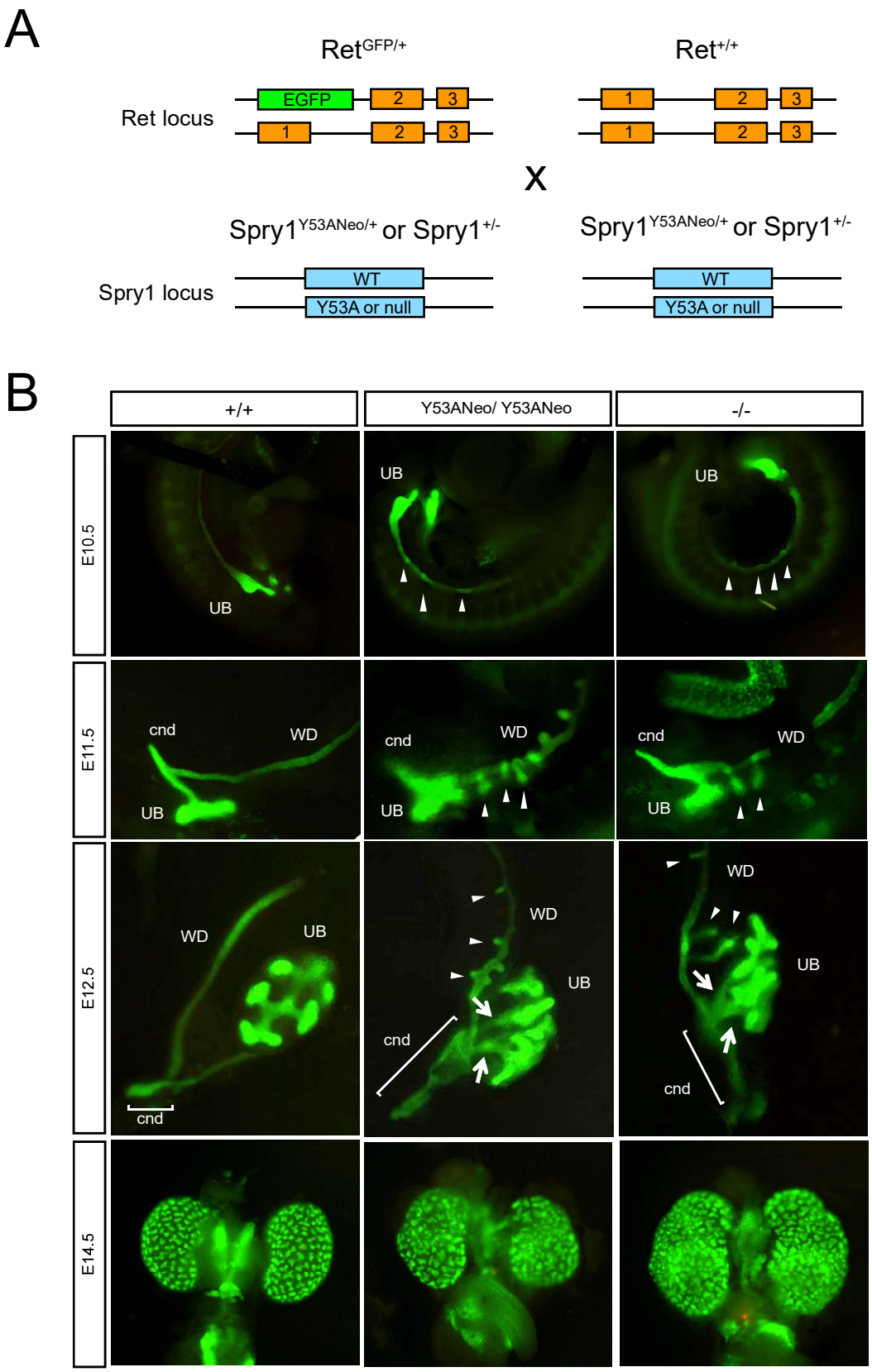
A
Ret^GFP/+
Ret^+/+
Ret locus
EGFP
1
2
3
X
Spry1^Y53ANeo/+ or Spry1^+/-
Spry1^Y53ANeo/+ or Spry1^+/-
Spry1 locus
WT
Y53A or null
B
+/+
Y53ANeo/ Y53ANeo
-/-
E10.5
E11.5
E12.5
E14.5
UB
cnd
WD

Figure 7. Vaquero et al.